PROTEINS: Structure, Function, and Genetics 43:395–402 (2001)

Free Energy Barrier Estimation of Unfolding the α-Helical Surfactant-Associated Polypeptide C

Ronen Zangi,[1] Helena Kovacs,[2,4] Wilfred F. van Gunsteren,[2] Jan Johansson,[3] and Alan E. Mark[1]*

[1]*Groningen Biomolecular Sciences and Biotechnology Institute (GBB), Department of Biophysical Chemistry, University of Groningen, Groningen, The Netherlands*

[2]*Laboratory of Physical Chemistry, Swiss Federal Institute of Technology, ETH Zentrum, Zurich, Switzerland*

[3]*Department of Medical Biochemistry and Biophysics, Karolinska Institutet, Stockholm, Sweden*

[4]*Bruker AG, Fällanden, Switzerland*

ABSTRACT **Molecular dynamics simulations were conducted to estimate the free energy barrier of unfolding surfactant-associated polypeptide C (SP-C) from an α-helical conformation. Experimental studies indicate that while the helical fold of SP-C is thermodynamically stable in phospholipid micelles, it is metastable in a mixed organic solvent of $CHCl_3/CH_3OH$/0.1 M HCl at 32:64:5 (v/v/v), in which it undergoes an irreversible transformation to an insoluble aggregate that contains β-sheet. On the basis of experimental observations, the free energy barrier was estimated to be ~100 kJ/mole by applying Eyring's transition state theory to the experimental rate of unfolding [Protein Sci 1998;7:2533–2540]. These studies prompted us to carry out simulations to investigate the unwinding process of two helical turns encompassing residues 25–32 in water and in methanol. The results give an upper bound estimation for the free energy barrier of unfolding of SP-C of ~20 kJ/mole. The results suggest a need to reconsider the applicability of a single-mode activated process theory to protein unfolding. Proteins 2001; 43:395–402.** © 2001 Wiley-Liss, Inc.

Key words: MD simulations; free energy barrier; α-SP-C; protein unfolding

INTRODUCTION

Lung epithelium synthesizes and excretes a surface-active material (surfactant) composed of a complex mixture of mainly phospholipids and specific proteins that reduces the surface tension at the air–liquid interface, preventing alveolar collapse at low lung volumes. Four surfactant-associated proteins—SP-A, SP-B, SP-C, and SP-D—have been described.[1] The properties of SP-C are of particular interest because of their clinical applications. The amino acid sequences of SP-C from seven animal species, ranging from mice to humans, show a conserved region of branched aliphatic residues (mainly valines). The amino acid sequence of porcine SP-C (LRIPCCPVNLKRLLVVVVVVVLVVVVIVGALLMGL), for example, contains 16 consecutive branched hydrophobic residues, of which 12 are valines. The three-dimensional (3-D) structure of SP-C has been determined by nuclear magnetic resonance (NMR) spectroscopy in $CHCl_3/CH_3OH$/0.1 M HCl at 32:64:5 (v/v/v).[2] The polypeptide fold is an α-helix comprising positions Asn9–Gly34. Based on the length of the helix and data from infrared (IR) spectroscopy,[3,4] it has been concluded that the α-helix spans the phospholipid bilayer.[5] In dodecylphosphocholine (DPC) micelles, native SP-C is very resistant to thermal unfolding. A synthetic peptide identical to SP-C does not, however, spontaneously adopt the native helical conformation,[6] and a dimeric SP-C fraction purified by Baatz et al.[7] was composed entirely of a β-sheet.

In vivo, SP-C is generated from a precursor of approximately 200 residues.[8] Once in a phospholipid environment α-helical SP-C is apparently stable, and there are suggestions that the α-helical conformation represents the global free energy minimum in this environment. Circular dichroism (CD), NMR, and Fourier transform infrared (FTIR) studies described by Szyperski et al.[9] strongly suggested that the helical fold in DPC micelles is thermodynamically stable. In a mixed organic solvent consisting of $CHCl_3/CH_3OH$/0.1 M HCl at 32:64:5 (v/v/v), a solvent that readily solubilizes SP-C in its native fold, however, α-helical SP-C slowly (within approximately 2 weeks) and irreversibly forms an aggregate with β-sheet structure.[9] Moreover, SP-C was recently shown to form amyloid fibrils, both in solution and in a lung disease in which proteins accumulate in the alveoli.[10]

Statistically, valines are underrepresented in the helical regions of soluble proteins and statistically based secondary structure prediction methods[11] predict SP-C to form a β-sheet. However, Li and Deber[12] have shown that the β-branched amino acids Val and Ile, in fact, rank among the best helix promoters in a membrane environment. This raises questions with regard to the intrinsic stability of the α-helical fold of SP-C and the factors that contribute to this stability both in vitro and in vivo.

NMR data indicate that the helical conformation of SP-C is not in a dynamic equilibrium with alternative nonhelical conformations in solution and that, once initiated,

Grant sponsor: Marie Curie Institute; Grant number: MCFI-1999-00161.

*Correspondence to: Alan E. Mark, Department of Biophysical Chemistry, University of Groningen, Nijenborgh 4, 9747 AG Groningen, The Netherlands. E-mail: a.e.mark@chem.rug.nl

Received 30 September 2000; Accepted 18 January 2001

unfolding and aggregation of SP-C in this solvent constitute a comparatively rapid, possibly concerted, process. Thus, in this solvent, the α-helical conformation is metastable with a significant barrier to unfolding. A high barrier to unfolding of α-helical SP-C was also suggested in previous simulation studies. The stability of the α-helix in a simulation of truncated SP-C in water at 500 K was striking as compared with results from other simulations at high temperatures of helical peptides or globular proteins.[13]

The role of the β-branched amino acids for contributing to the high barrier for helix-coil transition is apparent by noting that the time scale for folding/unfolding processes, for a model designed to represent water soluble helices of moderate length, is predicted to be <100 ns.[14] This analysis employed the Zimm–Bragg treatment of thermodynamic aspects of helix formation and results from free energy simulations of helix propagation for the barrier heights associated with the fundamental process of forming a helical hydrogen bond.

To analyze the α → β transformation of SP-C, Szyperski et al.[9] recorded a series of 2D TOCSY spectra in all-deuterated solvents at 283 K as a function of time. The decay constants of the cross-peaks between exchangeable backbone amide protons and side-chain protons for residues 13–27 in the α-helical portion of SP-C were found not to differ significantly from those of the cross-peaks between carbon-bound, nonexchangeable protons. Treating the unfolding of SP-C as a simple bimolecular activated reaction and applying Eyring's transition state theory to the unfolding rate constant yielded an estimate of 100 kJ/mole for the free energy barrier to global unfolding. Hydrogen-to-deuterium exchange rates were also used to suggest that the change in free energy associated with a local unfolding of the helix termini was within the range of 12–18 kJ/mole.

In a previous study,[13] molecular dynamics (MD) simulations performed in water, methanol, and chloroform were used to investigate the effect of the solvent environment on the stability of SP-C. These simulations indicated that the α-helical fold of the valine-rich region of SP-C was stable and that there is a significant barrier-to-helix unwinding. In this article, we investigate the barrier to unfolding directly by unwinding two helical turns encompassing residues 25–32, in water and in methanol environments.

COMPUTATIONAL DETAILS

The MD simulations were performed using the GROMACS package version 2.0[15,16] with the GROMOS96 (43A1) force field.[17] The solvent model is the simple point charge (SPC) model for water[18] and the GROMOS96 model for methanol.

To keep the system at a constant temperature of 300 K, a Berendsen thermostat[19] was applied, using a coupling time of 0.1 ps. The pressure was maintained by coupling to a reference pressure of 1 bar, with a coupling time of 1.0 ps and an isothermal compressibility of 4.6×10^{-5} bar^{-1}.[19] For the evaluation of the nonbonded interactions a twin range cutoff of 0.8 and 1.4 nm was used. Interactions within the larger cutoff were updated every 5 steps. The time step used was 0.002 ps. Water bond distances and angles were constrained using the SETTLE algorithm,[20] while the methanol and the protein were constrained using the SHAKE algorithm[21] with a tolerance of 5×10^{-5}.

TABLE I. Constraint Lengths and Minimal Simulation Times for SP-C Simulation in Water and in Methanol, Incorporating a Distance Constraint Between C_α (Val25) and C_α (Leu32)

Solvent	Water	Methanol
Constraint length interval for relaxation (nm)	0.01	0.02
Relaxation time (ps)	10	10
Constraint length interval for averaging (nm)	0.02	0.04
Equilibration time (ps)	100	200
Averaging time (ps)	100	200

To investigate the behavior of SP-C in the two solvents, two 5.0-ns simulations, one in water and one in methanol, were carried starting from the NMR structure determined by Johansson et al.[2]

To obtain an estimate of the free energy barrier, a distance constraint was imposed between the C_α of residues Val25 and Leu32. This part of SP-C spans two helical turns composed of residues Val-Val-Ile-Val-Gly-Ala-Leu-Leu. The average equilibrium value of the distance between the C_α of Val25 and Leu32 is 1.05 nm. The constraint on this distance was extended to 2.45 nm and contracted down to 0.97 nm. Before applying the constraint, the system was equilibrated for 500 ps. At each constraint length, the system was equilibrated and the data collected. At the midpoint of the constraint length interval, the system was relaxed for a short period of time. Constraint length intervals, relaxation time, equilibration time, and averaging time in water and in methanol for the constrained SP-C simulations are presented in Table I.

The averaging time is the minimum averaging time that was used. For certain constraint lengths, longer simulations (200–500 ps) were used to determine the mean force acting along the constraint to ensure convergence.

An estimation of the error in the mean force along the constraint was obtained using the block averaging method. The data produced during the averaging time were divided into blocks of size n; averages were calculated for each block. The set of average values was considered an independent data set, and the standard deviation of the mean taken as the error estimate of that set. Convergence is indicated when the error estimate as a function of the block size n remains constant. The value of the height of this plateau is taken as an estimate for the error.

The integration of the mean force to obtain the free energy profile was performed using the trapezoidal rule. As this profile is a relative free energy, it was shifted so that the minimum of the curve was at zero. Since the relative uncertainty in the constraint length is much smaller than the relative uncertainty in the mean force along the constraint, the estimated error of the free energy profile was performed by integrating the errors of the

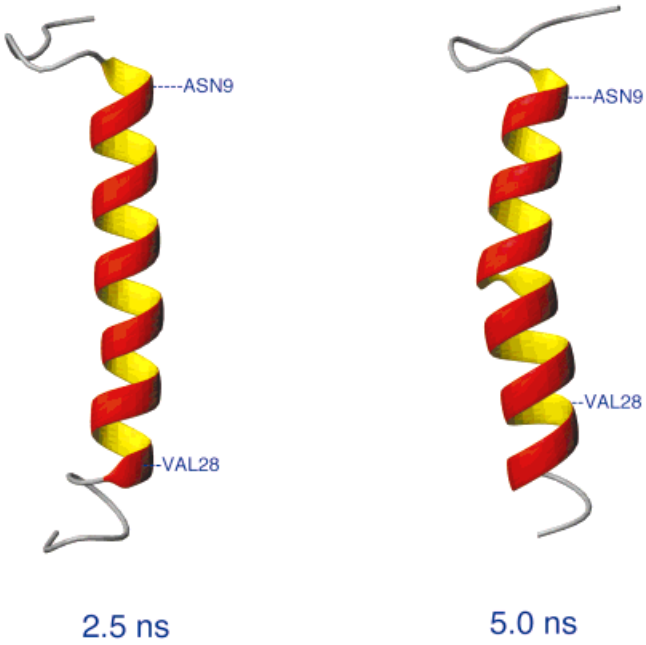

Fig. 1. Structure of SP-C in water after 2.5- and 5.0-ns simulation time.

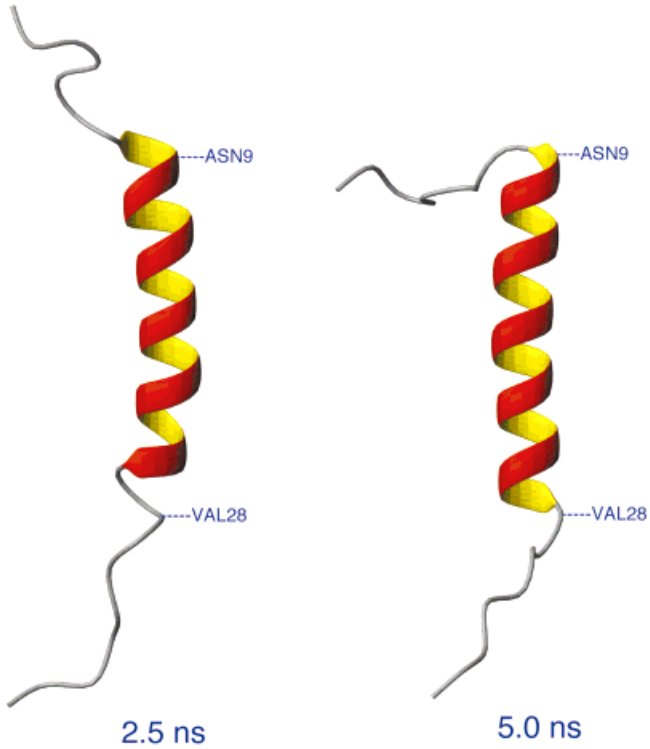

Fig. 2. Structure of SP-C in methanol after 2.5- and 5.0-ns simulation time.

mean force where the reference point (for the accumulation of the errors) is at the minimum of the curve.

A cubic box of 1.5-nm minimum distance between the protein and the box walls was used to ensure that, even after full extension (~1.4 nm) of the backbone between the two C_α, the protein did not directly interact with its periodic image, given the cutoff. The resulting number of solvent molecules was 12,294 and 5,667 for water and methanol, respectively. Residues Arg2, Lys11, and Arg12 as well as the N- and the C-terminals were protonated (as the experimental mixed organic solvent was slightly acidic), yielding $+4e$ for the total charge.

RESULTS

Relative Stability of SP-C in Water and in Methanol

Starting from the NMR structure of SP-C[2] in a mixed organic solvent of $CHCl_3/CH_3OH$/0.1 M HCl at 32:64:5 (v/v/v), two simulations were carried out to infer the stability of SP-C. Figures 1 and 2 show two structures of SP-C in water and in methanol, respectively, after simulating for periods of 2.5 ns and 5.0 ns. It is evident that the α-helical fold of SP-C from residue Asn9 to Ile28 is stable over this period in the simulation. As proposed previously,[13] the α-helix structure of SP-C is rigid because of the cooperative packing structure formed by the hydrophobic β-branched side-chains. Segment Val28–Leu32 is locally unfolded in methanol, whereas in water it preserves, to some degree, an α-helical structure.

It has been proposed that helix unfolding proceeds by solvent insertion and replacement of the α-helical hydrogen bonds.[22] Disruption of the backbone hydrogen bonds is presumed also to be required for proton exchange.[23] Table II displays the average number of neighboring solvent

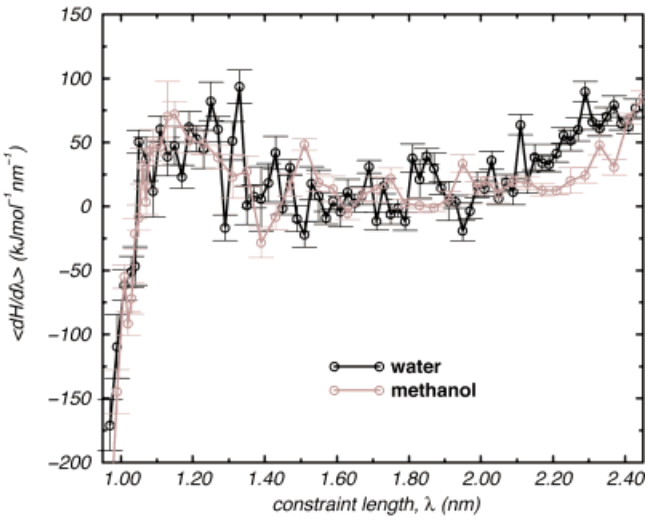

Fig. 3. Mean force, $\left\langle \frac{\partial H}{\partial \lambda} \right\rangle$, acting along the constraint as a function of the constraint length for the simulation in water and for the simulation in methanol. Vertical lines represent the estimated error.

atoms within a radius of 0.4 nm around each backbone amide proton site for the simulations in water and in methanol. Table II also displays the decay rates of the NMR signal from backbone amide hydrogens due to exchange.[9] The values for the average number of neighboring solvent atoms should be compared only within each solvent, as they have not been corrected for the different density of atoms of the pure solvents. Despite the differ-

TABLE II. Average Number of Neighboring Solvent Atoms Around the Backbone Amide Hydrogens of SP-C Within a Solvation Sphere of 0.4-nm Radius*

Residue	Water	Methanol	k_{NH}	Residue	Water	Methanol	k_{NH}
Leu1	7.5	11.9	—	Val20	0.5	0.2	2.3
Arg2	4.3	5.3	—	Val21	0.4	0.2	2.0
Ile3	3.7	4.3	—	Leu22	0.4	0.3	0.0
Cys5	5.0	5.1	—	Val23	0.7	0.4	0.0
Cys6	3.8	4.2	—	Val24	0.2	0.2	1.2
Val8	3.5	4.8	—	Val25	0.4	0.2	0.8
Asn9	2.8	3.9	—	Val26	0.3	0.1	1.0
Leu10	1.3	2.9	14.7	Ile27	0.2	0.2	0.9
Lys11	0.1	1.4	2.7	Val28	0.2	0.7	3.3
Arg12	1.1	0.8	3.3	Gly29	1.8	4.8	5.2
Leu13	0.9	0.3	1.2	Ala30	2.0	3.8	31.7
Leu14	0.3	0.2	0.7	Leu31	0.4	4.5	10.8
Val15	0.7	0.3	0.5	Leu32	0.8	4.2	25.9
Val16	0.6	0.2	2.1	Met33	1.1	4.3	—
Val17	0.5	0.1	1.6	Gly34	3.2	6.0	—
Val18	0.3	0.2	1.6	Leu35	3.2	5.4	—
Val19	0.3	0.2	1.3				

*The value is determined over the 5.0-ns trajectory. Backbone amide proton exchange rates, k_{NH} (in units of 10^{-5} min^{-1}), determined from decay rates of $H^{\alpha,\beta}/HN$ NMR signals (reproduced from [9] by subtracting the decay rate of carbon-bound protons from the observed decay rates) are displayed in the last column. It is estimated that $k_{NH} > 1 \times 10^{-2}$ min^{-1}, where no reading is given.

ence in the time length sampled in the NMR experiment, as compared with the simulation time length, the number of the neighboring solvent atoms from the simulation and the decay rates of the NMR signals is correlated. The segment of Leu13–Ile27 has very low values of neighboring solvent atoms, indicating that the backbone is essentially inaccessible to the solvent. This segment corresponds to the residues that have low values of proton exchange rate, k_{NH}. For the simulations in water, the region of residues with low values of neighboring solvent atoms can be viewed as extended to Leu32, with the exception of residues Gly29 and Ala30. These residues interrupt the sequence of the β-branched amino acids; thus, small solvent molecules (e.g., water) are closer to the backbone amide hydrogens.

Estimation of the Barrier to Unfolding

To estimate the free energy barrier to unfolding, an unfolding pathway must be imposed on the system. A distance constraint (λ) between the C_α of residues Val25 and Leu32 was chosen to serve as such a pathway. These residues encompass two turns of the helix. Residues Val25–Ile27, which are part of the valine-rich segment, show very low values of neighboring solvent atoms and very high protection of the amide protons, i.e., very low values of k_{NH} (Table II). Residues Val28–Leu32 form the second last turn of the helix. This is the last turn for which there is a significant protection of the amide protons, and it exhibits greater fluctuations in the backbone dihedral angles than does the valine-rich segment of the helix. It may be reasonably assumed that the unwinding of this turn of the helix is an early event in the unfolding process. The unfolding path chosen will not necessarily correspond to the path of the lowest free energy. The simulations provide only an upper bound to the height of the barrier.

The average force acting along the direction of the constraint was determined for a series of constraint distances (Fig. 3). Starting at a distance of 1.05 nm, which corresponds to the actual distance obtained as an average when equilibrating the NMR structure for 500 ps, the constraint distance was increased stepwise, until a fully extended conformation was reached at 2.45 nm. The constraint was also contracted to 0.97 nm. The free energy as a function of the imposed unfolding reaction coordinate (or the potential of mean force) is the integral of the mean force acting along the constraint and is shown in Figures 4 and 5 for water and methanol, respectively. Note that the average force acting along the constraint, and thereby the free energy profile, are not corrected for possible metric tensor effects. Metric tensor effects arise from the transformation from Cartesian to internal coordinates and are likely to result in overestimation of the constraint force at larger distances.

The simulations yield an estimate for the barrier height of the free energy of 19 ± 10 kJ/mol in water and 23 ± 9 kJ/mol in methanol. The minimum of the free energy profile occurred at a constraint length ~1.05 nm. In the simulations in water, at a constraint length of ~1.49 nm, the turn of the helix between residues Val28–Leu32 unwinds, and all the hydrogen bonds between those residues are broken and replaced by those with water molecules. The plateau region from this point to a constraint length of 1.75 nm represents an extension of this segment. Further increase of the constraint length shows a second barrier, which is a result of unwinding the part of the helix composed of residue Val25–Ile27. From a constraint length of 2.00 nm, the free energy rises rapidly as the peptide segment is forced to adopt an entropically unfavorable linear conformation. In the simulations in methanol, unwinding of the constrained part of the helix also starts

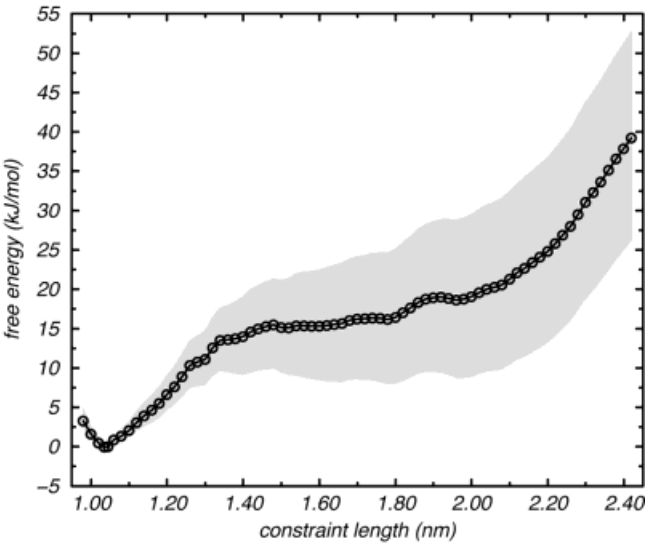

Fig. 4. Free energy profile for unwinding two turns of the helix between residues Val25 and Leu32 in water. The curve is shifted such that the minimum is at zero height. The shaded area is the accumulated uncertainty in the profile from the minimum of the curve.

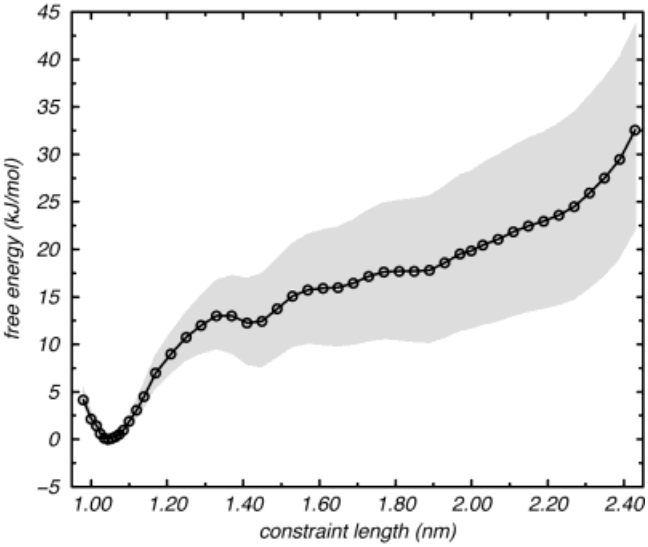

Fig. 5. Free energy profile for unwinding two turns of the helix between residues Val25 and Leu32 in methanol. The curve is shifted so that the minimum is at zero height. The shaded area is the accumulated uncertainty in the profile from the minimum of the curve.

from the C-terminal part with several small barriers. At a constraint length of ~1.35 nm, the hydrogen bonds involving residues Ala30–Leu32 are broken and that part of the helix unwinds. Further increase of the constraint length to ~1.55 nm results in unwinding the segment Val28–Leu32. At a constraint length of 1.79 nm the helical structure is unfolded up to residue Ile27. Only at a constraint length of 2.21 nm are the intra-helix hydrogen bonds involving Val26 and Val25 broken. At this point, the constrained segment is fully extended.

SP-C structures at several constraint lengths are shown in Figures 6 and 7 for the simulations in water and in methanol, respectively. Although the free energy profiles in both solvents are very similar, there are some differences in the structures of the SP-C as the constraint length is increased. In the simulation with water, by imposing the constraint, the N-terminal segment (Leu1–Val8) interacts with the α-helix part of the peptide, and it is not free to move in the solution. In addition, one of the helix hydrogen bonds, at around Val17, is broken and replaced by hydrogen bonds with water molecules. In the simulation with methanol the N-terminal part of the peptide (Leu1–Val8) is free and no loss of α-helical hydrogen bonds in the valine-rich region is observed.

DISCUSSION

The barrier to unfolding of the α-helix is related to the cooperative packing of the amino acid side chains in the valine-rich segment. Independent of the solvent, the backbone hydrogen bonds essentially experience a hydrophobic environment. To initiate unfolding of the helix, interactions between the closely packed valine side-chains or the backbone hydrogen bonds must be disrupted. In both solvents, the backbone atoms of the helical residues Lys11–Val28 are effectively inaccessible to the solvent (Table II). Furthermore, the segment Val28–Leu32 is shown to preserve the α-helical structure in water but not in methanol. In a more polar solvent, the packing of the hydrophobic side-chains is expected to be enhanced, because of hydrophobic effects. However, it is not possible to attribute directly to a particular set of interactions, either the stability of the peptide, or the height of the barrier to unfolding.[24] In a predominantly hydrophobic environment such as the interior of the DPC micelles, it would be expected that SP-C exhibits a significant degree of flexibility. Experimentally, it is found that in DPC micelles SP-C is very resistant to thermal denaturation with a melting point exceeding 363 K.[5] Loss of helicity as a function of increasing temperature is observed but no cooperative melting. The effects of heating are partially reversed on cooling. From the simulations, however, it is not possible to comment on whether or not the α-helical fold is thermodynamically stable in a hydrophobic environment.

In $CHCl_3/CH_3OH$/0.1 M HCl at 32:64:5 (v/v/v), α-helical SP-C is metastable with respect to a nonhelical aggregated gel. From the rate of loss of NMR signals, the barrier to global unfolding has been estimated[9] at ~100 kJ/mol. Based on Eyring's theory, this estimate treats unfolding as a one-step activated bimolecular reaction with a transmission rate probability of 1.0. To estimate the free energy barrier to unfolding from the simulations we have calculated the free energy profile along one possible unfolding pathway, namely as a function of the distance between the C_α of Val25 and Leu32. The free energy barrier for unwinding those two turns of the helix in methanol and in water was estimated to be ~20 kJ/mol. The extension of the estimation of the barrier height to unfolding the entire helix is based on the experimental observation that when starting from the α-helical structure, no other state possesses exchangeable backbone amide protons for residues Leu13–Ile27; rather, once initiated, the unfolding of the

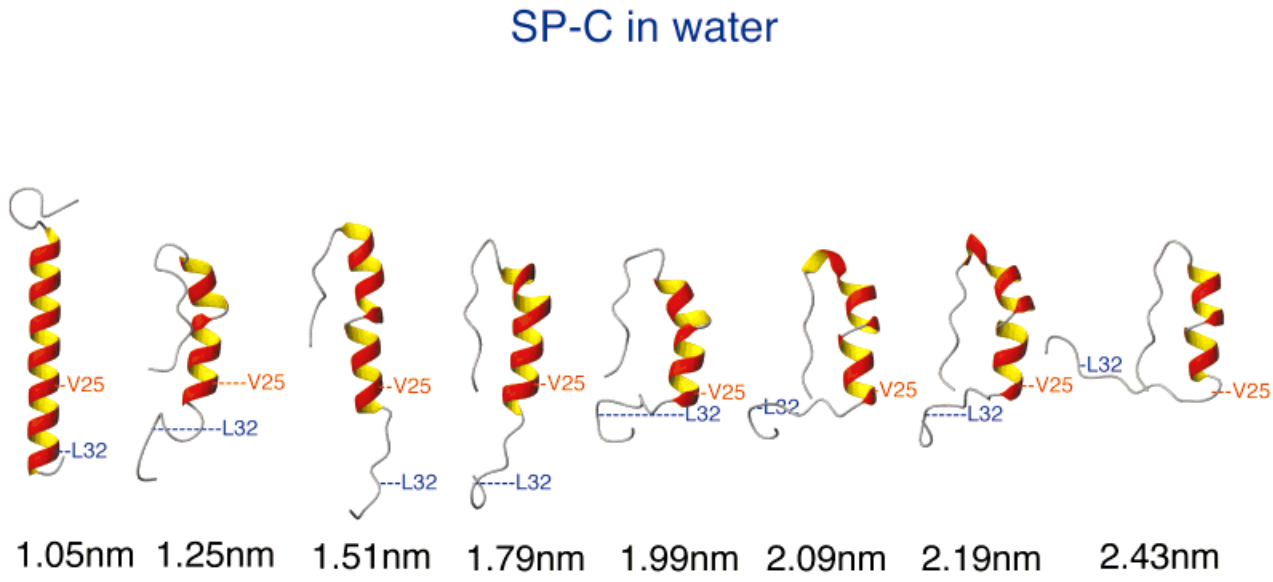

Fig. 6. Structure of SP-C in water for eight values of the constraint length that correspond to an extension of 0.00–1.38 nm in the distance between the C_α of residues Val25 and Leu32.

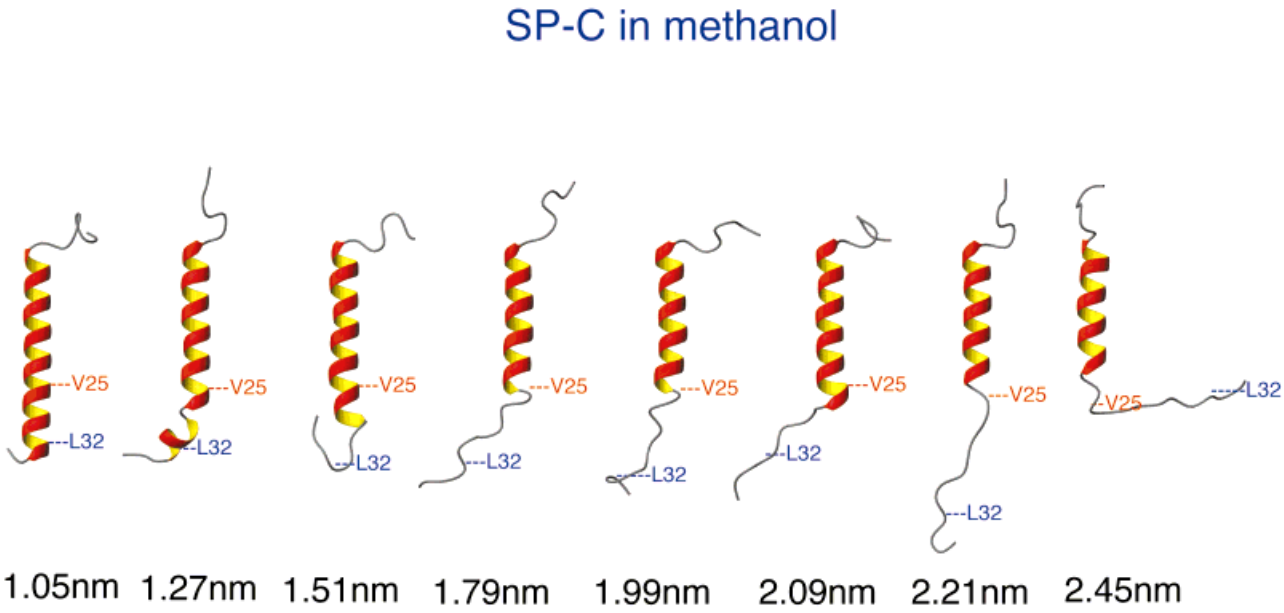

Fig. 7. Structure of SP-C in methanol for eight values of the constraint length that correspond to an extension of 0.00–1.40 nm in the distance between the C_α of residues Val25 and Leu32.

peptide is both rapid and complete. As the imposed unfolding pathway does not necessarily correspond to the real unfolding pathway, the estimation of the free energy barrier for unfolding is only an upper bound to the real barrier.

This estimate of 20 kJ/mol for the free energy barrier from the simulations is considerably less than that suggested by Szyperski et al.[9] There are several possible reasons for this difference. First, the simulations may not give the appropriate barrier height. This could be due to the force field parameterization used or to the fact that the pure solvents used (water and methanol) in simulations were not identical to the solvent used in the experiments. It should be noted, in this regard, that the solvent used in the NMR experiments is itself quite polar, with the molar ratio $CHCl_3/CH_3OH/H_2O$ approximately 3:11:2. Furthermore, work by Brooks and Nilsson[25] on the unfolding of a blocked alanine tripeptide indicates that the helix-promoting ability in different solvents follows the order methanol > methanol–water > water, and that the range in height of the free energy barrier is 3–11 kJ/mol, with the higher value observed in methanol and the lower value in water. By contrast, our work does not show any significant difference between the value estimated for the free energy

barrier in the two solvents, although a difference in the helix–coil thermodynamics in the two solvents may exist. Also as Brooks and Nilsson noted, the model tripeptide system may not reflect the additive contributions in longer peptides.

Another source of inaccuracy in determining the free energy barrier can be due to the force field parameters, although it is unlikely that the force field alone accounts for such a discrepancy. Therefore, it must be questioned whether the application of Eyring's theory or other transition state theories in protein unfolding is appropriate. Certainly, protein unfolding is not a simple bimolecular reaction, nor does it necessarily proceed along a single pathway. The application of transition state theory assumes that unfolding is a concerted process in which the system surmounts a specific energy barrier that traverses a specific path. It is unlikely that the entire peptide unwinds as a single activated process. Instead, the loss of a specific turn(s) may be thought of as triggering the subsequent unwinding of the remainder of the helix. The question is whether this can be considered an activated process with a defined transition state. As long as the barrier to remove the next turn is comparable to the preceding barriers, an intermediate will not accumulate to a concentration detectable by NMR. An initial unfolding event could potentially occur at several different places along the helix. Fraying, for example, is seen at both ends of the helix.

The overall rate of loss of helical SP-C from solution will depend on the nature of the free energy barrier along a specific reaction coordinate, the probability of finding the system moving along that particular coordinate, and a diffusive component, depending on the nature of the specific path taken by a specific molecule. The diffusive component and the fact that unfolding may occur only via a certain set of restricted pathways are not considered when estimating the barrier height based on Eyring's theory assuming a transmission rate of 1.0. When converting a rate to a free energy barrier, Eaton et al.[26] proposed the use of a scaling factor of 1×10^6 s^{-1} to account for diffusion in protein folding instead of $k_BT/h = 6 \times 10^{12}$ s^{-1}. As the unfolding process is not a reaction governed by quantum mechanics, the use of k_BT/h as the prefactor in the transition-state formula seems unwarranted. Moreover, a value of 10^{12} s^{-1} implies that when started from the top of the barrier the peptide would unfold within 1 ps. Using a value of 10^6 s^{-1} would lower the barrier estimated from the rate of unfolding by approximately 40 kJ/mol.

Szyperski et al.[9] have estimated the difference in the free energy associated with local unfolding of the terminal residues. This estimate was based on the ratio between the rate of exchange of the backbone amide protons of these residues compared with the rate of exchange expected if their amide protons were fully exposed to solvent. It was assumed that effectively no exchange occurred in the helical conformation and that the helical conformation was in equilibrium with a conformation in which the amide protons are fully exposed to solvent. The difference in the free energy of unfolding residues Val28–Leu32 was estimated at 12–17 kJ/mol. This is comparable to the difference in free energy between the helical and extended conformations of about 15 kJ/mol found in our simulation at about constraint length of 1.49 nm in water and at ~1.55 nm in methanol.

In conclusion, our results show that for proteins, the fact that unfolding appears to be a concerted process with no intermediates does not imply the reaction can be treated in terms of simple transition state theory. The search for an appropriate reaction coordinate in systems characterized by a large number of degrees of freedom will inevitably lead to slower kinetics. Thus, the application of transition state theory will lead to a server overestimation of the free energy barrier. In fact, in complex systems, unless details of the nature of the transition state are known, estimations of the free energy barrier based on the rate of unfolding provides no additional insight or information then the rate of unfolding itself.

ACKNOWLEDGMENTS

This research has been supported by a Marie Curie Fellowship of the European Community, programme Human Potential, under contract number MCFI-1999-00161.

REFERENCES

1. Goerke J. Pulmonary surfactant: functions and molecular composition. Biochim Biophys Acta 1998;1408:79–89.
2. Johansson J, Szyperski T, Curstedt T, Wüthrich K. The NMR structure of the pulmonary surfactant-associated polypeptide SP-C in an apolar solvent contains a valyl-rich α-helix. Biochemistry 1994;33:6015–6023.
3. Pastrana B, Mautone AJ, Mendelsohn R. Fourier transform infrared studies of secondary structure and orientation of pulmonary surfactant SP-C and its effect on the dynamic surface properties of phospholipids. Biochemistry 1991;30: 10058–10064.
4. Vandenbussche G, Clercx A, Curstedt T, Johansson J, Ruysschaert JM. Structure and orientation of the surface-associated protein C in a lipid bilayer. Eur J Biochem 1992;203:201–209.
5. Johansson J, Szyperski T, Wüthrich K. Pulmonary surfactant-associated polypeptide SP-C in lipid micelles: CD studies of intact SP-C and NMR secondary structure determination of depalmitoyl-SP-C (1–17). FEBS Lett 1995;362:261–265.
6. Johansson J, Nilsson G, Strömberg R, Robertson B, Jörnvall H, Curstedt T. Secondary structure and biophysical activity of synthetic analogs of the pulmonary surfactant polypeptide SP-C. Biochem J 1995;307:535–541.
7. Baatz JE, Smyth KL, Whitsett JA, Baxter C, Absalom DR. Structure and functions of a dimeric form of surfactant protein SP-C: a Fourier transform infrared and surfactometry study. Chem Phys Lipids 1992;63:91–104.
8. Beers MF, Kim CY, Dodia C, Fisher A. Localization, synthesis and processing of surfactant protein SP-C in rat lung analyzed by epitope-specific antipeptide antibodies. J Biol Chem 1994;269: 20318–20328.
9. Szyperski T, Vandenbussche G, Curstedt T, Ruysschaert J-M, Wüthrich K, Johansson J. Pulmonary surfactant-associated polypeptide C in a mixed organic solvent transforms from a monomeric α-helical state into β-sheet aggregates. Protein Sci 1998;7:2533–2540.
10. Gustafsson M, Thyberg J, Näslund J, Eliasson E, Johansson J. Amyloid fibril formation by pulmonary surfactant protein C. FEBS Lett 1999;464:138–142.
11. Rost B, Sander C. Combining evolutionary information and the neural networks to predict protein secondary structure. Proteins 1994;19:55–72.
12. Li S-C, Deber CM. A measure of helical propensity for amino acids in membrane environments. Nature Struct Biol 1994;1:368–373.
13. Kovacs H, Mark AE, Johansson J, van Gunsteren WF. The effect

of environment on the stability of an integral membrane helix: molecular dynamics simulations of surfactant protein C in chloroform, methanol and water. J Mol Biol 1995;247:808–822.
14. Brooks CL. Helix–coil kinetics: folding time scales for helical peptides from a sequential kinetic model. J Phys Chem 1996;100: 2546–2549.
15. Berendsen HJC, van der Spoel D, van Drunen R. GROMACS: a message-passing parallel molecular dynamics implementation. Comp Phys Commun 1995;91:43–56.
16. van der Spoel D, Hess B, Feenstra KA, Lindahl E, Berendsen HJC. GROMACS user manual version 2.0. Groningen, The Netherlands: Nijenborgh AG; 1999. http://md.chem.rug.nl/~gmx.
17. van Gunsteren WF, Billeter SR, Eising AA, Hünenberger PH, Krüger P, Mark AE, Scott WRP, Tironi IG. Biomolecular simulation: GROMOS96 manual and user guide. Groningen, The Netherlands: BIOMOS BV; 1996.
18. Berendsen HJC, Postma JPM, van Gunsteren WF, Hermans J. Interaction models for water in relation to protein hydration. In: Pullman B, editor. Intermolecular forces. Dordrecht, The Netherlands: D. Reidel; 1981. p 331–342.
19. Berendsen HJC, Postma JPM, van Gunsteren WF, DiNola A, Haak JR. Molecular dynamics with coupling to an external bath. J Chem Phys 1984;81:3684–3690.
20. Miyamoto S, Kollman PA. SETTLE: an analytical version of the SHAKE and RATTLE algorithms for rigid water models. J Comp Chem 1992;13:952–962.
21. Ryckaert JP, Ciccotti G, Berendsen HJC. Numerical integration of the Cartesian equations of motion of a system with constraints; molecular dynamics of *n*-alkanes. J Comp Phys 1977;23:327–341.
22. Tirado-Rives J, Jorgensen WL. Molecular dynamics simulations of the unfolding of an α-helical analogue of ribonuclease A S-peptide in water. Biochemistry 1991;30:3864–3871.
23. Englander SW, Sosnick TR, Englander JJ, Mayne L. Mechanisms and uses of hydrogen exchange. Curr Opin Struct Biol 1996;6:18–23.
24. Mark AE, van Gunsteren WF. Decomposition of the free energy of a system in terms of specific interactions: implications for theoretical and experimental studies. J Mol Biol 1994;240:167–176.
25. Brooks CL, Nilsson L. Promotion of helix formation in peptides dissolved in alcohol and water–alcohol mixtures. J Am Chem Soc 1993;115:11034–11035.
26. Eaton WA, Thompson PA, Chan C-K, Hagen SJ, Hofrichter J. Fast events in protein folding. Structure 1996;4:1133–1139.